Eur. Phys. J. Appl. Phys. **93**, 10903 (2021)

https://doi.org/10.1051/epjap/2020200315

THE EUROPEAN PHYSICAL JOURNAL APPLIED PHYSICS

Regular Article

# Critical behavior of $Pr_{0.65}Sr_{0.35}MnO_3$ compound investigated by a Monte Carlo Simulation★

Lhaj El Hachemi Omari[1,*], Abdelmajid Lekdadri[1], Rachid Chami[2], and El Kebir Hlil[3]

[1] University Hassan II of Casablanca, LPMMAT, Faculty of Sciences Ain Chock, Maarif B.P 5366, Morocco
[2] University Hassan II of Casablanca, LEPE, High School of Technology, Oasis B.P 8112, Morocco
[3] Univ. Grenoble Alpes, CNRS, Grenoble INP, Institut Néel, 38000 Grenoble, France

Received: 4 October 2020 / Received in final form: 29 November 2020 / Accepted: 7 December 2020

**Abstract.** The critical behavior and magnetic properties of $Pr_{0.65}Sr_{0.35}MnO_3$ (symbolized here by PSMO) were studied using Monte Carlo Simulation (MCS). The thermal bath algorithm and Ising model in which exchange interactions via the third nearest neighbor were used to calculate the magnetic and magneto-caloric properties. The effects of temperature ($T$) and external magnetic field ($h$) on the magnetic behavior of PSMO were examined. The results show that the Curie temperature ($T_C$) is close to the experimental value. The magnetic entropy shows a maximum value around the $T_C$ that increases linearly with the increase of the external field. The critical behavior of the PSMO compound was studied by analyzing the magnetization isotherms and by exploiting Arrott plots. The obtained values of the critical exponents are $\beta = 0.336$, $\gamma = 1.121$, and $\delta = 4.335$. These values are very close to those reported for the 3D-Ising model. The variation of maximum magnetic entropy ($\Delta S_m^{max}$) and relative cooling power (RCP) around the Curie temperature were calculated; the obtained values of $\Delta S_m^{max}$ and those of RCP ranging from 3.612 and 92.7 for 1T to 6.191 and 209.9 for 5T, respectively. These results are sufficiently interesting to consider the PSMO compound as a promising candidate for magnetic refrigeration.

## 1 Introduction

In recent years, a great attention has been paid to the perovskite-type of materials, in particular the manganite-based compounds [1,2], due to their interesting properties such as those of optics, ferroelectricity, ferromagnetism and not only the magnetocaloric (MC).

It is important to mention that magnetic refrigeration has found wide applications in energy-intensive industrial and commercial refrigerators such as large-scale air conditioners, heat pumps, supermarket refrigeration units, waste separation, chemical processing, gas liquification, liquor distilling, sugar refining, grain drying, and so forth [3,4]. In addition, uniform distribution of the magnetic entropy change is very desirable for Ericsson-cycle-based magnetic refrigerators. The large magnetic entropy change induced by a relatively low magnetic field change is beneficial for household application of active magnetic refrigerant materials [5].

The discovery of superconducting oxides in 1987 intensified research in the field of magnetic oxides. In 1993, following the discovery of giant magnetoresistance (variation of the resistivity in the presence of a magnetic field) in manganese-based perovskites. For instance, the magnetic oxides of $LnMnO_3$, $Ln_2MnO_4$ type (where Ln is a rare earth element) made a subject of numerous studies [6–10]. In addition to its magneto-resistive behavior, manganite compounds present important MC properties (i.e. variation of the entropy under the effect of a magnetic field) [11]. The MC effect of this type of material is one of the results of great change in magnetic entropy ΔS due to the large spontaneous magnetization change at the Ferromagnetic-Paramagnetic (FM-PM) transition [12]. Understanding the nature of the PM-FM transition is important to fully reveal the MC effect in the vicinity of the transition point. As the process of the FM-PM transition is governed by the corresponding critical exponents (CE), therefore the study of CE in the asymptotic critical region, located over and below $TC$ of the 2nd order PM-FM phase transition, is a powerful tool for in-depth analysis of the mechanisms of the microscopic magnetic interaction responsible for this transition [13,14]. Near the Curie temperature, in the double exchange model in the framework of the long-range mean field theory [15], it has been reported that the critical parameters of based-manganese oxides are linked to the PM-FM transition. However, Pramanik et al. have predicted that CE in manganite compounds are consistent with the short-range exchange interaction model [16].

In the case of mixed Mn-valences in $La_{1-x}A_xMnO_3$ or $Ln_{2-x}A_xMnO_4$ manganite type, the studies carried out since 1950 by Jonker and in 2011 by Tlili et al. [11] have

★ Contribution to the Topical Issue "Advanced Materials for Energy Harvesting, Storage, Sensing and Environmental Engineering (ICOME 2019)", edited by Mohammed El Ganaoui, Mohamed El Jouad, Rachid Bennacer, Jean-Michel Nunzi.

* e-mail: bophysiq@gmail.com

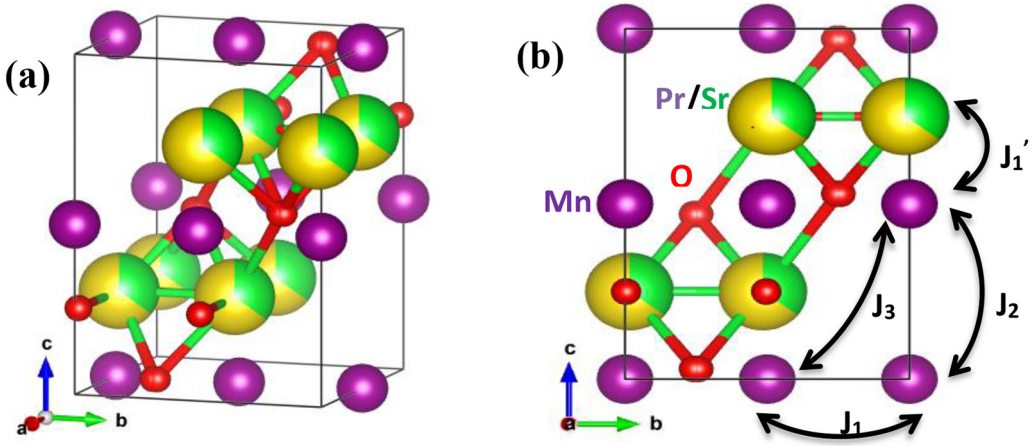


**Fig. 1.** (a) Crystalline structure of the studied system. (b) Various kinds of the considered exchange interactions.

shown an insulating antiferromagnetic behavior for low values of $x$ and a metallic ferromagnetic behavior for $x$ over 0.1. This behavior has been explained by the double exchange mechanism proposed by Zener [17]. The half-metallic ferromagnetic compound $PrMnO_3$ has been widely studied in the literature by first principles calculations [18], and the Monte Carlo Simulation [19] and experimentally by structural and magnetic measurements [20].

To create a mixture of ionic valence as $Mn^{3+}/Mn^{4+}$, that is very interesting for the specific magnetocaloric behavior in the manganite derived compounds by the double-exchange interaction between $Mn^{+3}/Mn^{+4}$ ions via oxygen ion [17]. For that, the compound $PrMnO_3$ has been doped with a bi-valent $M^{2+}$. For example, the $Sr^{2+}$, $Ca^{2+}$ and $Ba^{2+}$ doping with a specific level lead to the promising materials in a particular application [2,6,21–23]. But the compounds with the level $x = 1/3$ in the formula $Pr_{1-x}Sr_xMnO_3$ have attracted more attention due to their interesting properties near room temperature, such as the Curie temperature $T_C = 295$ K [2].

In the present work, the temperature and external magnetic field effects, on the magnetic and magneto-caloric properties and also on the critical behavior in the manganite oxide $Pr_{0.65}Sr_{0.35}MnO_3$, were studied by means of the MCS. The modified Arrott plots (APM) [24] and the isothermal magnetization diagrams were used to studying the critical behavior of this compound. The found results were compared with those reported in the literature.

## 2 Theoretical model

The perovskite structure of PSMO will be modeled by a periodic three-dimensional sub-lattice (Fig. 1a) in which the magnetic ions ($Pr^{3+}$, $Mn^{4+}$ and $Mn^{3+}$) are located at sites ($i$). Each site $i$ carries a spin moment $S_i$ so that the spin of $Mn^{3+}$ is $S = 2$, the spin of $Mn^{4+}$ is $S = 3/2$, and the spin of $Pr^{3+}$ is $\sigma = 1$. For a perfect structure, the Mn elements have a mixed valence are $Mn^{4+}$ with a probability of 0.35 and $Mn^{3+}$ with a probability of 0.65.

Magnetic energy encompasses the exchange interactions between the spins up to the third nearest neighbor, as well as the interactions of the spins with the external magnetic field $h$. This energy is given in the context of the Ising model as follows:

$$H = -\left( J_1 \sum_{i,j} S_i S_j + J_2 \sum_{i,k} S_i S_k + J_3 \sum_{i,m} S_i S_m + J_1' \sum_{i,l} S_i \sigma_l + h \left( \sum_i S_i \sum_l \sigma_l \right) \right) \quad (1)$$

where $\langle i,j \rangle$, $\langle i,k \rangle$, and $\langle i,m \rangle$ represent, respectively the sum of the first, second and third closest sites to the site $i$. $J_1$, $J_2$, and $J_3$ are the parameters of exchange interaction between Mn-Mn ions. $J_1'$ is the exchange interaction between Mn-Pr ions.

### 2.1 Monte Carlo Simulation (MCS)

The simulation of the above model by means of the MCS method was based on the sampling algorithm of thermal baths within the framework of the statistical distribution of Boltzmann [25]. The simulation program was built to scan all the sites of the magnetic sub-lattice successively so that at each site by making attempts to reverse a single spin. The manganese ion sub-lattice is simulated by a cubic box with a total number of spins $N = L^3$, where L being the number of sites ($i$) in each of the three directions of the cubic box, the thermodynamic limit being determined at $L = 20$. In order to reproduce the infinite size of the system studied the periodic boundary conditions were chosen. The initial configuration was generated randomly. The statistical stability of the calculation has been reached when the program takes a number of MC steps. Consequently, $5 \times 10^4$ MCS steps per spin have been used to obtain reliable results throughout this calculation. To reach the equilibrium, the first $2 \times 10^4$ steps have been eliminated and then the statistical measurements of physical magnitudes were made on the last $3 \times 10^4$ steps.

The different types of exchange interactions between the magnetic ions are shown in Figure 1b. Each manganese ion has three types of exchange interactions [26]: $J_1$ the exchange interactions with the first close neighbors as well as that with the second ($J_2$) and with the third ($J_3$) near neighbors. The first interaction between the praseodymium ion with the manganese one is taken into account and symbolized by $J'_1$, while the interaction between the praseodymium ions has been considered negligible. The coordination number for each interaction order $J_1$, $J_2$, $J_3$ and $J'_1$ are 2, 4, 8 and 2, respectively.

After equilibrium, each physical quantity was calculated by scanning the last $3.10^4$ MCS steps. The average value of each quantity was estimated with respect of temperature or external magnetic field, and given as a density by site.

The density of the magnetization is given by:

$$M = \frac{1}{N}\left\langle \sum_i S_i \right\rangle. \tag{2}$$

Magnetic susceptibility is estimated by the equation:

$$\chi = \beta' N\left(\langle M^2\rangle - \langle M\rangle^2\right) \tag{3}$$

with $(\beta')^{-1} = k_B T$ and $k_B$ is the Boltzmann constant.

The isothermal variation of the magnetic entropy $\Delta S_M$ of the PSMO material could be estimated from:

$$\Delta S_m(T,h) = S_m(T,h) - S_m(T,0). \tag{4}$$

The relative cooling power (RCP) can be estimated by the equation:

$$RCP = \int_{T_i}^{T_f} \Delta S_m(T)dT. \tag{5}$$

The $T_i$ and $T_f$ are respectively the edges of initial and final temperature of the half-maximum of $\Delta S_m$.

## 3 Results and discussions

### 3.1 Phase transition

In a first step, the effect of the cluster size (L) on the magnetic properties of the PSMO would be optimized, indeed the thermal variation of the magnetization M(T) at zero magnetic field ($h = 0$) have been calculated for different values of $L$. The calculation shows that the Curie temperature ($T_C$) increases with the increase in the $L$ value up to a threshold value ($L_C = 20$) at which $T_C$ reaches its saturation value. Consequently, above the critical value ($L > L_C$), the cluster reproduces the massive behavior of the studied material.

The thermal variation of magnetization calculated for PSMO studied with an external field of zero ($h = 0$) for the optimal size of $L = 20$ is shown in Figure 2. This curve shows a ferromagnetic-paramagnetic (FM-PM) phase transition during heating. From the minimum value, of $dM/dT$ as a function of $T$, the value of $T_C$ is estimated about 297 K, which is comparable to the experimental value reported by Sankarrajan et al. [27] (298 K) and by Guillou et al. [28] (295 K) for of $Pr_{0.65}Sr_{0.35}MnO_3$.

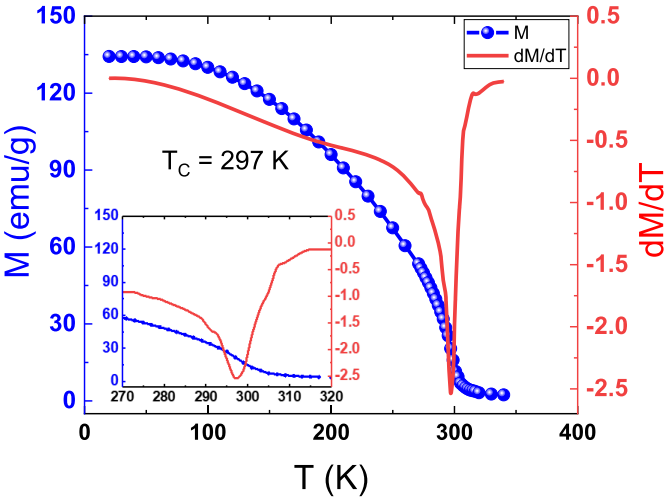


**Fig. 2.** Thermal magnetization of PSMO calculated for $h = 0$ and $L = 20$.

The theoretical effective magnetic moment has been deduced by means of equation (7) [29] from the effective magnetic moments of the manganese ions $Mn^{3+}$, $Mn^{4+}$ and $Pr^{3+}$ which are, respectively, equal to $\mu_{eff}(Mn^{3+}) = 4.91\ \mu_B$ with pseudo spin $S = 2$, and $\mu_{eff}(Mn^{4+}) = 3.87\ \mu_B$ with pseudo spin $S = 3/2$ [30] and $\mu_{eff}(Pr^{3+}) = 3.58\ \mu_B$ with pseudo spin $S = 1$ [29]:

*See equation (6) below.*

The resulting value of the total magnetic moment is $\mu^{th}_{eff} = 5.407\mu_B$. The found values of $\mu_{eff}$ and $\mu^{th}_{eff}$ are according to the experimental results given in Table 1.

From the effective moment, $M_{sat}$ could be estimated using the following equation:

$$\mu_{eff} = \frac{M_{sat}.M_{mol}}{5558}. \tag{7}$$

The obtained value is 134.7 emu/g, which corresponding to the value of $M_{sat}$ at $T = 20$ K in Figure 2. This value is very close to that reported in the literature [21,29,31–34] as shown in Table 1.

### 3.2 Critical exponents

The critical exponents (CE), near the temperature of the second order magnetic phase transition can be defined by the following relationships [35]:

$$\mu^{th}_{eff} = \sqrt{0.65 \times \left(\mu_{eff}(Pr^{3+})\right)^2 + 0.65 \times \left(\mu_{eff}(Mn^{3+})\right)^2 + 0.35 \times \left(\mu_{eff}(Mn^{4+})\right)^2}. \tag{6}$$

**Table 1.** Magnetic and magnetocaloric parameters of PSMO.

| Composition | $T_C$ (K) | $\mu_{eff}$ ($\mu_B$) | $\mu_{eff}^{th}$ ($\mu_B$) | $\mu_0 H$ (T) | $-\Delta S_m^{max}$ (J/kg.K) | $RCP$ (J/kg) | References |
|---|---|---|---|---|---|---|---|
| $Pr_{0.67}Sr_{0.33}MnO_3$ | 317 | 5.69 | 5.44 | – | – | – | [29] |
| $Pr_{0.6}Sr_{0.4}MnO_3$ | 292 | – | – | 5 | 4.85 | 223.29 | [31] |
| $Pr_{0.6}Sr_{0.4}MnO_3$ | 286 | 5.51 | 3.95 | 3 | 2.41 | 151.16 | [21] |
| $Pr_{0.67}Sr_{0.33}MnO_3$ | 261 | 5.71 | 4.24 | 3 | 2.36 | 119.42 | [21] |
| $Pr_{0.63}Sr_{0.37}MnO_3$ | 305 | 5.81 | – | 5 | 8.52 | – | [32] |
| $Pr_{0.6}Sr_{0.4}MnO_3$ | 320 | – | – | 2.5 | 2.3 | 34.5 | [33] |
| $La_{0.67}Sr_{0.33}MnO_3$ | 370 | 3.7 | 4.4 | 5 | 3.67 | 173.4 | [34] |
| PSMO | 297 | 5.407 | 5.407 | 1 | 3.612 | 92.7 | This work |
| | | | | 5 | 6.191 | 209.9 | |

the spontaneous magnetization exponent (beta $\beta$) is defined by:

$$M(T > T_C, h \to 0) = M_0 \left(\frac{T - T_C}{T_C}\right)^{\beta} \quad (8)$$

were $M_0$ is the critical magnetization amplitude.

In order to estimate the value of $\beta$, the change in $Ln(M)$ as a function of $Ln((T - T_C) / T_C)$ was calculated in the paramagnetic region ($T > T_C$) without an external field ($h = 0$), (Fig. 3a). The obtained value of $\beta$, which deduced from the slope of this curve, is $\beta = 0.336$.

The isothermal magnetic susceptibility exponent (gamma $\gamma$) is given by:

$$\chi_0^{-1}(T < T_C, h \to 0) = \frac{h_0}{M_0}\left(\frac{T - T_C}{T_C}\right)^{\gamma} \quad (9)$$

where, $T_C$ is the critical temperature and $\chi_0^{-1}$ is the inverse of the initial susceptibility. We have plotted the variation of $Ln(\chi_0^{-1})$ as a function of $Ln((T - T_C) / T_C)$ over the transition point at $h = 0$ as shown in Figure 3b, the fit of this curve is well linear and the derived $\gamma$ value is $\gamma = 1.121$.

The critical isothermal exponent (delta $\delta$) near the transition point is given by:

$$M(T = T_C, h) = D_0(h)^{\frac{1}{\delta}} \quad (10)$$

were $D_0$ is a critical field amplitude, and $h$ is the applied magnetic field ($h = \mu_0 H$).

These CE are linked to each other by the following relationship:

$$\delta = 1 + \frac{\gamma}{\beta}. \quad (11)$$

The change of $ln(M)$ versus $ln(h)$ is plotted in Figure 3c for the purpose of determining the value of $\delta$, the linear adjustment allows to deduce the $\delta$ values as 4.71 at 297 K and 3.95 at 299 K. These values are not so far to that calculated from equation (11) which gives the result of $\delta$ as 4.335.

Frequently, four models can be generated according to the values of CE [35] which are: 3D-Ising model, 3D-Heisenberg, effective mean field, and tri-critical mean field model.

The derived values of the critical exponents are in good agreement with the values found for similar systems (Tab. 2). Since they are close to those known for the universal model: 3d-Ising. It is noted that the values of critical exponents near $T_C$, obtained from MCS, correspond with reasonable agreement with the matching values obtained from the 3D-Ising approach, indicating that long-distance interactions dominate the critical behavior around $T_C$ in this system, which may be explained by the perfectly distribution of the spins derived from different ions.

### 3.3 Arrott plots

In order to determine the magnetic transition nature, the Arrott model was used. Based on the magnetization isotherms near the transition temperature $T_C$ (Fig. 4a), the curves which show the variation of $(h/M)$ as a function of $M^2$ are illustrated in Figure 4b. These plots have a linear behavior with high values of the magnetic field $(h)$ in which for the temperature $T = T_C$ the extrapolation of that curve must pass through the origin. The curves of $(H/M) = f(M^2)$ show a profile of Arrott diagram characteristic of a 2nd order phase transition around the temperature 299 K.

This criterion is derived from the fact that the thermodynamic equilibrium is reached when the internal energy is minimal. Indeed, the free energy $G$ can be developed in terms of the order parameter $M$ as follows:

$$G(T, M) = G_0 + \frac{1}{2}A(T)M^2 + \frac{1}{4}B(T)M^4 - hM. \quad (12)$$

Parameters A and B are temperature dependent parameters. The equilibrium conditions are described by the two conditions; $\left(\frac{\partial G}{\partial M}\right) = 0$ and $\left(\frac{\partial^2 G}{\partial M^2}\right) > 0$, which allows to extract a linear dependence between $(h/M)$ and $M^2$

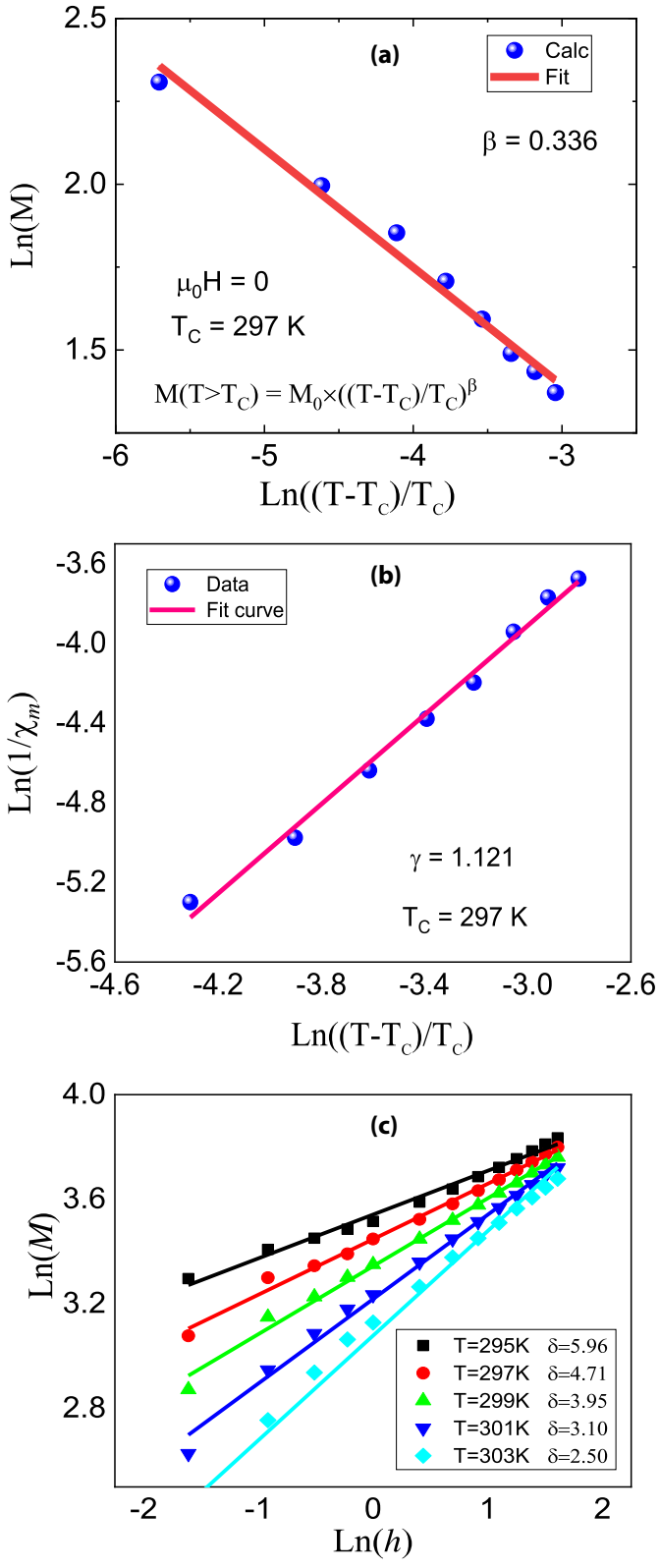


**Fig. 3.** (a) Change of $Ln(M)$ versus $Ln((T-T_C)/T_C)$ in the paramagnetic region for $h=0$. (b) Variation of $Ln(\chi_0^{-1})$ versus Ln $((T-T_C)/T_C)$ for $T>T_C$ at $h=0$. (c) Variation of $Ln(M)$ versus $Ln(h)$, the symbols represent the calculated data and the solid lines represent their fits.

as follows:

$$\frac{h}{M} = A(T) + B(T)M^2. \tag{13}$$

The study of the sign of the parameters A and B allowed deducing the nature and the temperature of transition. The parameter A is positive above $T_C$, zero for $T=T_C$ and negative below $T_C$. Moreover, the parameter B is positive in the case of the second order transition and negative in the case of the first order transition [37,38]. The variation of A and B as a function of temperature around $T_C$ is presented in Figure 5. These plots show that the parameter A increases from a value of −0.239 T.g/emu at $T=269$ K to a positive value of 0.078 T.g/emu at $T=315$ K and changes the sign at the temperature 299 K. Also, the parameter B shows positive values, situated between $9.86\times10^{-3}$ and $11.52\times10^{-3}$ T.g$^3$/emu$^3$, for all studied values of $T$. This confirms that the PSMO system undergoes a 2nd order phase transition at the temperature 299 K.

### 3.4 Magnetic entropy & RCP

As magneto-calorie is one of the attractive magnetic properties of this compound, the applied magnetic field effect on the magnetic entropy has been studied. Indeed, the MCS was exploited in which the magnetic entropy $\Delta S_m$ was varied by the variation of the external magnetic field. Then, the magnetic entropy $\Delta S_m$ $(h,T)$ was calculated using equation (4) mentioned in the previous section. The thermal variation of $\Delta Sm$ for a series of $h$ values is plotted in Figure 6a.

Figure 6a shows the thermal variation curves of $\Delta S_m$ $(h,T)$ for various applied magnetic field values for the PSMO sample. The curve $\Delta S_m$ $(h,T)$, rises to a maximum value $\left(\Delta S_m^{max}\right)$ around 299 K. These patterns are asymmetrical to the left and the right of $T_C$, which is intended for a second-order phase transition.

The maximum $\Delta S_m^{max}$ curve vary linearly from 3.612 J/kg.K for $h=1$T up to 6.191 J/kg.K for $h=5$T (Fig. 6b). On the other hand, the efficiency of magnetic cooling can be measured by the characteristic quantity RCP, defined in equation (5). The estimated RCP values are shown in Figure 6b. The RCP plot follows a quasi linear increase with applied magnetic field change. The RCP values increase from 92.7 J/kg for $h=1$T up to and 209.9 J/kg for 5T.

As the $\Delta S_m^{max}$ and RCP variations are quasi linear relative to the applied field variation, this change can be adjusted by the following two equations:

$$\Delta S_m^{max} = D_1 h^{n_1} \tag{14}$$

$$RCP = D_2 h^{n_2}. \tag{15}$$

The adjusted parameters by using equations (14) and (15) are $n_1=0.34$, $n_2=0.51$, $D_1=3.49$ and $D_2=90.9$. The obtained values of $\Delta S_m^{max}$ and PCR are in agreement with those reported in the literature (Tab. 1). These results are sufficiently interesting to consider the PSMO compound as a promising candidate for magnetic refrigeration.

**Table 2.** The list of critical exponent values.

| Model/Composition | $\beta$ | $\gamma$ | $\Delta$ | References |
|---|---|---|---|---|
| 3D-Ising model | 0.325 | 1.241 | 4.82 | [35] |
| Tricritical Mean field | 0.25 | 1 | 5 | [35] |
| Mean field model | 0.365 | 1.336 | 4.80 | [35] |
| 3D-Heisenberg model | 0.5 | 1.0 | 3.0 | [35] |
| $La_{0.7}Sr_{0.3}MnO_3$ | 0.45 | 1.08 | 3.4 | [36] |
| $La_{0.67}Sr_{0.33}MnO_3$ | 0.306 | 1.178 | 4.025 | [38] |
| PSMO | 0.336 | 1.121 | 3.95–4.71 | This work |

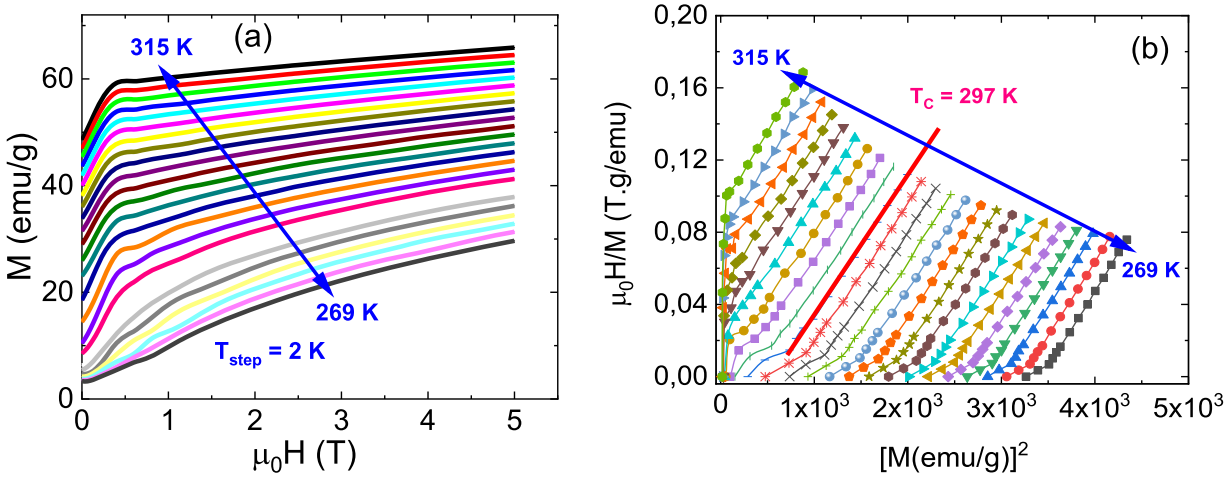


**Fig. 4.** (a) Isothermal magnetization curves, and (b) Arrott plots in the proximity of $T_C$.

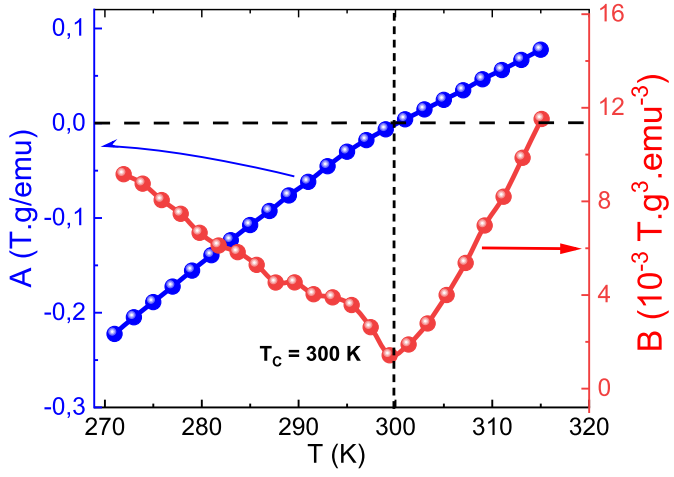


**Fig. 5.** Variation of the thermal parameters A and B versus temperature around $T_C$.

## 4 Conclusion

In summary, the magnetic properties, critical exponents and magnetocaloric properties of PSMO perovskite have been studied using Monte Carlo Simulation. The studied system shows a 2nd order FM-PM magnetic transition at $T_C = 297$ K. The maximum entropy ($\Delta S_m^{max}$) and the relative cooling power (RCP) have been estimated and found to increase with the external field. The estimation of the critical exponent values has been made on the basis of different methods such as Arrott plot method and critical isothermal analysis. The obtained critical exponents are in

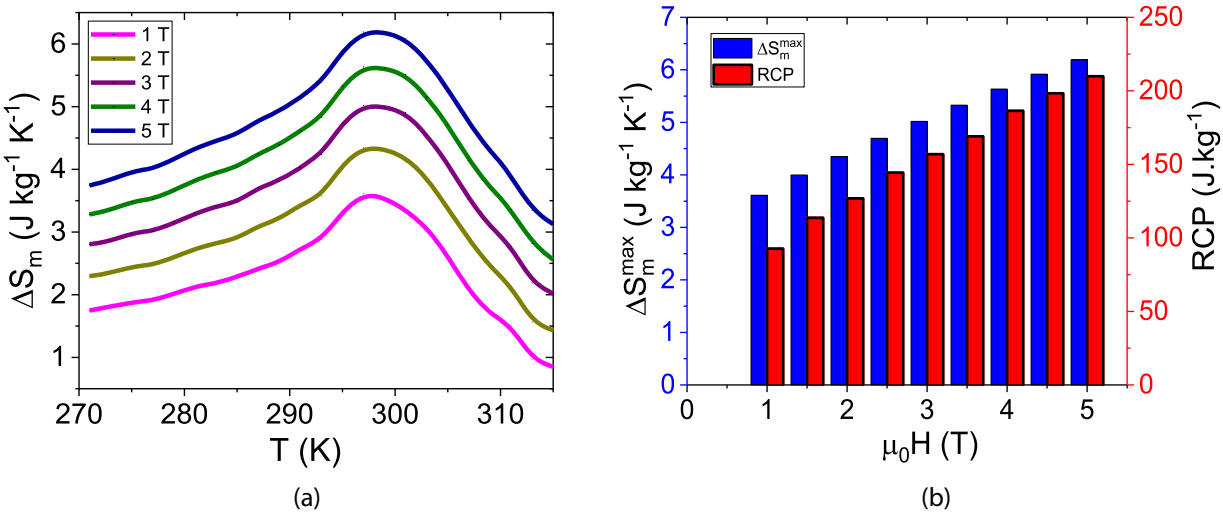


**Fig. 6.** (a) Thermal variation of $\Delta S_m$ for a series of the external magnetic field $h$. (b) Variation of $\left(\Delta S_m^{max}\right)$ and RCP versus $h$ around $T_C$.

good agreement with the literature. The obtained results of $\Delta S_m^{max}$ and PCR are sufficiently interesting to consider the PSMO compound as a promising candidate for magnetic refrigeration devices.

## Author contribution statement

Lhaj El Hachemi Omari: conceptualization, computation, formal analysis, writing - preliminary draft, writing – review & editing Abdelmagid Lekdadri: formal analysis, investigation & writing - preliminary draft preparation. Rachid Chami: visualization & data acquisition. El-Kebir Hlil: validation, supervision & writing – review.

## References


1. J.Q. Li, J. Appl. Phys. **90**, 637 (2001)
2. N. Panwar, A. Rao, R.S. Singh, W.K. Syu, N. Kaurav, Y.-K. Kuo, S.K. Agarwal, J. Appl. Phys. **104**, 083906 (2008)
3. V.K. Pecharsky, K.A. Gschneidner, A.O. Tsokol, Rep. Prog. Phys. **68**, 1479 (2005)
4. E. Bruck, J. Phys. D: Appl. Phys. **38**, R381 (2005)
5. M.-H. Phan, S.-C. Yu, J. Magn. Magn. Mater. **308**, 325 (2007)
6. R. Von Helmolt, J. Wecker, B. Holzafel, L. Schultz, K. Samwer, Phys. Rev. Lett. **71**, 2331 (1993)
7. A. Zouari, C. Boudaya, E. Dhahri, Phys. Status Solidi A **188**, 1177 (2001)
8. A. Urushibara, Y. Moritomo, T. Arima, A. Asamitsu, G. Kido, Y. Tokura, Phys. Rev. B **51**, 14103 (1995)
9. J. Inoue, S. Maekawa, Phys. Rev. Lett. **74**, 3407 (1995)
10. K. Cherif, J. Dhahri, E. Dhahri, M. Oumezzine, H. Vincent, J. Solid State Chem. **163**, 466 (2002)
11. M.T. Tlili, N. Chihaoui, M. Bejar, E. Dhahri, M.A. Valente, E.K. Hlil, J. Alloys Compd. **509**, 6447 (2011)
12. M.H. Phan, S.C. Yu, N.H. Hur, Appl. Phys. Lett. **86**, 072504 (2005)
13. A. Tozri, E. Dhahri, E.K. Hlil, M.A. Valente, Solid State Commun. **151**, 315 (2011)
14. Ma. Oumezzine, O. Pena, S. Kallel, Mo. Oumezzine, J. Alloys Compd. **539,** 116 (2012)
15. M. Seeger, S.N. Kaul, H. Kronmüller, R. Reisser, Phys. Rev. B **51**, 12585 (1995)
16. A.K. Pramanik, A. Banerjee, Phys. Rev. B **79**, 214426 (2009)
17. C. Zener, Phys. Rev. **82**, 403 (1951)
18. B. Bouadjemi, S. Bentata, A. Abbad, W. Benstaali, B. Bouhafs, Solid State Commun. **168**, 6 (2013)
19. M. Oumarou, N. Aknin, N. Mohamedou, M.L. Ould Ne, Int. J. Sci. Eng. Res. **7**, 1836 (2016)
20. K.P. Lim, S.A. Halim, S.K. Chen, S.W. Ng, J.K. Wong, H.M. Albert Gan, H.S. Woon, AIP Conf. Proceed. **1328**, 241 (2011)
21. A.K. Saw, G. Channagoudra, S. Hunagund, R.L. Hadimani, V. Dayal, Mater. Res. Express **7**, 016105 (2020)
22. V. Dayal, S. Keshri, Solid State Commun. **142**, 63 (2007)
23. L.A. Dubraja, D. Wang, T. Brezesinski, Cryst. Eng. Comm. **20**, 245 (2018)
24. A. Arrott, J.E. Noakes, Phys. Rev. Lett. **19**, 786 (1967)
25. H.N. Motlagh, G. Rezaei, J. Magn. Magn. Mater. **445**, 26 (2018)
26. J. Tikkanen, M. Geilhufe, M. Frontzek, W. Hergert, A. Ernst, P. Paturi, L. Udby, J. Phys.: Condens. Matter **28**, 036001 (2016)
27. S. Sankarrajan, K. Sakthipandi, V. Rajendran, Phase Transitions **85**, 427 (2001)
28. F. Guillou, U. Legait, A. Kedous-Lebouc, V. Hardy, EPJ Web Conf. **29**, 00021 (2012)
29. S. Hcini, S. Zemni, A. Triki, H. Rahmouni, M. Boudard, J. Alloys Compd. **509**, 1394 (2011)
30. H.E. Stanley, *Introduction to Phase Transitions and Critical Phenomena* (Oxford University Press, London, 1971)
31. R. M'nassri, W. Cheikhrouhou-Koubaa, N. Boudjada, A. Cheikhrouhou, EPJ Web Conf. **29**, 00051 (2012)

32. M.H. Phan, H.X. Peng, S.C. Yu, J. Appl. Phys. **97**, 10M306 (2005)
33. S. Zemni, M. Baazaoui, J. Dhahri, H. Vincent, M. Oumezzine, Mater. Lett. **63**, 489 (2009)
34. L.H. Omari, A. Lekdadri, E.K. Hlil, H. Lassri, R. Moubah, A. Tozri, E. Dhahri, M. Kerouad, A. Zaim, Mater. Today Commun. **23**, 2352 (2020)
35. W.J. Lu, X. Luo, C. Y. Hao, W.H. Song, Y.P. Sun, J. Appl. Phys. **104**, 113908 (2008)
36. M. Ziese, J. Phys.: Condens. Matter **13**, 2919 (2001)
37. B.K. Banerjee, Phys. Lett. **12**, 16 (1964)
38. C.M. Bonilla, F. Bartolomé, L.M. García, M. Parra-Borderías, J. Herrero-Albillos, J. Appl. Phys. **107**, 09E131 (2010)

**Cite this article as**: Lhaj El Hachemi Omari, Abdelmajid Lekdadri, Rachid Chami, El Kebir Hlil, Critical behavior of $Pr_{0.65}Sr_{0.35}MnO_3$ compound investigated by a Monte Carlo Simulation, Eur. Phys. J. Appl. Phys. **93**, 10903 (2021)